EDGE GUIDED GANS WITH CONTRASTIVE LEARNING FOR SEMANTIC IMAGE SYNTHESIS

Anonymous authors
Paper under double-blind review

ABSTRACT

We propose a novel edge guided generative adversarial network with contrastive learning (ECGAN) for the challenging semantic image synthesis task. Although considerable improvement has been achieved, the quality of synthesized images is far from satisfactory due to three largely unresolved challenges. 1) The semantic labels do not provide detailed structural information, making it difficult to synthesize local details and structures. 2) The widely adopted CNN operations such as convolution, down-sampling, and normalization usually cause spatial resolution loss and thus cannot fully preserve the original semantic information, leading to semantically inconsistent results (e.g., missing small objects). 3) Existing semantic image synthesis methods focus on modeling 'local' semantic information from a single input semantic layout. However, they ignore 'global' semantic information of multiple input semantic layouts, i.e., semantic cross-relations between pixels across different input layouts. To tackle 1), we propose to use edge as an intermediate representation which is further adopted to guide image generation via a proposed attention guided edge transfer module. Edge information is produced by a convolutional generator and introduces detailed structure information. To tackle 2), we design an effective module to selectively highlight class-dependent feature maps according to the original semantic layout to preserve the semantic information. To tackle 3), inspired by current methods in contrastive learning, we propose a novel contrastive learning method, which aims to enforce pixel embeddings belonging to the same semantic class to generate more similar image content than those from different classes. By doing so, it can capture more semantic relations by explicitly exploring the structures of labeled pixels from multiple input semantic layouts. Experiments on three challenging datasets show that our ECGAN achieves significantly better results than state-of-the-art methods.

1 INTRODUCTION

Semantic image synthesis refers to generating photo-realistic images conditioned on pixel-level semantic labels. This task has a wide range of applications such as image editing and content generation (Chen & Koltun, 2017; Isola et al., 2017; Park et al., 2019; Gu et al., 2019; Bau et al., 2019a;b; Liu et al., 2019; Qi et al., 2018; Jiang et al., 2020; Tang et al., 2020a). Although existing approaches conducted interesting explorations, we still observe unsatisfactory aspects mainly in the generated local structures and details, as well as small-scale objects, which we believe are mainly due to three reasons:

1) Conventional methods (Park et al., 2019; Wang et al., 2018; Liu et al., 2019) generally take the semantic label map as input directly. However, the input label map provides only structural information between different semantic-class regions and does not contain any structural information within each semantic-class region, making it difficult to synthese rich local structures within each class. Taking label map S in Fig. 1 as an example, the generator does not have enough structural guidance to produce a realistic bed, window, and curtain from only the input label (S).

2) The classic deep network architectures are constructed by stacking convolutional, down-sampling, normalization, non-linearity, and up-sampling layers, which will cause the problem of spatial resolution losses of the input semantic labels.

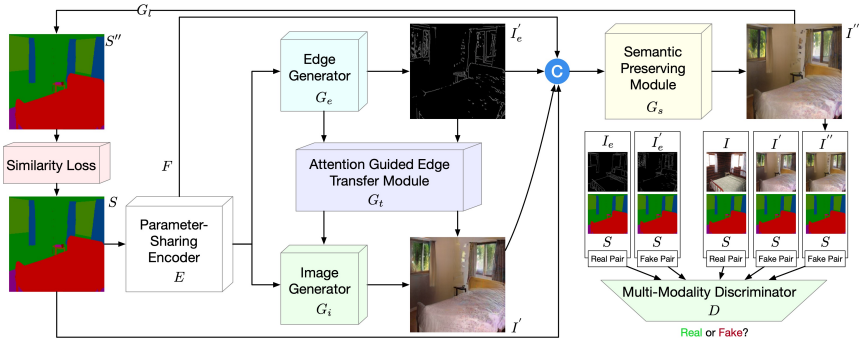

Figure 1: Overview of the proposed framework. It consists of a parameter-sharing encoder E, an edge generator G_e, an image generator G_i, an attention guided edge transfer module G_t, a label generator G_l, a similarity loss module, a contrastive learning module G_c (not shown for simplicity), and a multi-modality discriminator D. Both G_e and G_i are connected by G_t from two levels, i.e., edge feature-level and content-level, to generate realistic images. G_s is proposed to preserve the semantic information of the input semantic labels. G_l aims to transfer the generated image back to the label for calculating the similarity loss. G_c tries to capture more semantic relations by explicitly exploring the structures of labeled pixels from multiple input semantic layouts. D aims to distinguish the outputs from two modalities, i.e., edge and image. The whole framework can be end-to-end trained so that each component can benefit from each other. The symbol © denotes channel-wise concatenation.

3) Existing methods for this task are typically based on global image-level generation. In other words, they accept a semantic layout containing several object classes and aim to generate the appearance of each one using the same network. In this way, all the classes are treated equally. However, because different semantic classes have distinct properties, using specified network learning for each would intuitively facilitate the complex generation of multiple classes.

To address these three issues, in this paper, we propose a novel edge guided generative adversarial network with contrastive learning (ECGAN) for semantic image synthesis. The overall framework of ECGAN is shown in Fig. 1.

To tackle 1), we first propose an edge generator to produce the edge features and edge maps. Then the generated edge features and edge maps are selectively transferred to the image generator and improve quality of the synthesized image by using our attention guided edge transfer module.

To tackle 2), we propose an effective semantic preserving module, which aims at selectively highlighting class-dependent feature maps according to the original semantic layout. We also propose a new similarity loss to model the relationship between semantic categories. Specifically, given a generated label S'' and corresponding ground truth S, similarity loss constructs a similarity map to supervise the learning.

To tackle 3), a straightforward solution would be to model the generation of different image classes individually. By so doing, each class could have its own generation network structure or parameters, thus greatly avoiding the learning of a biased generation space. However, there is a fatal disadvantage to this. That is, the number of parameters of the network will increase exponentially with the number of semantic classes, which will cause memory overflow and make it impossible to train the model. To further address this limitation, we propose a pixel-wise contrastive learning method, which lifts the current image-wise training strategy to an inter-image, pixel-to-pixel paradigm. It essentially learns a well-structured pixel semantic embedding space by making full use of the global semantic similarities among labeled layouts. Moreover, we explore image generation from a class-specific context, which we believe is beneficial for generating richer details compared with the existing image-level generation methods. A new class-specific pixel generation strategy is proposed for this purpose. It can effectively handle the generation of small objects and details, which are common difficulties encountered by the global-based generation.

With the proposed ECGAN, we achieve new state-of-the-art results on Cityscapes (Cordts et al., 2016), ADE20K (Zhou et al., 2017), and COCO-Stuff (Caesar et al., 2018) datasets, demonstrating the effectiveness of our approach in generating images with complex scenes, and showing significantly better results compared with state-of-the-art methods.

2 RELATED WORK

Edge Guided Image Generation. Edge maps are usually adopted in image inpainting (Ren et al., 2019; Nazeri et al., 2019a; Li et al., 2019) and image super-resolution (Nazeri et al., 2019b) tasks to reconstruct the missing structure information of the inputs. For example, Nazeri et al. (2019a) proposed an edge generator to hallucinate edges in the missing regions given edges, which can be regarded as an edge completion problem. Using edge images as the structural guidance, EdgeConnect (Nazeri et al., 2019a) achieves good results even for some highly structured scenes. Moreover, Pix2pix (Isola et al., 2017) adopts edge maps as input and aims to generate realistic shoes and handbags, which can be seen as an edge-to-image translation problem. Unlike previous works, including EdgeConnect (Nazeri et al., 2019a), we propose a novel edge generator to perform a new task, i.e., semantic label-to-edge translation. To the best of our knowledge, we are the first to generate edge maps from semantic labels. Then the generated edge maps, with more local structure information, can be used to improve the quality of the image results.

Semantic Image Synthesis aims to generate a photo-realistic image from a semantic label map (Wang et al., 2018; Chen & Koltun, 2017; Qi et al., 2018; Park et al., 2019; Liu et al., 2019; Bansal et al., 2019; Zhu et al., 2020a; Ntavelis et al., 2020; Zhu et al., 2020b; Tang et al., 2020b; Sushko et al., 2021; Tan et al., 2021b;a; Zhu et al., 2020b). With the semantic information as guidance, existing methods have achieved promising performance. However, we can still observe unsatisfying aspects, especially on the generation of the small-scale objects, which we believe is mainly due to the problem of spatial resolution losses associated with deep network operations such as convolution, normalization, and down-sampling, etc. To solve this problem, Park et al. (2019) proposed GauGAN, which uses the input semantic labels to modulate the activations in normalization layers through a spatially-adaptive transformation. However, the spatial resolution losses caused by other operations such as convolution and down-sampling have not been resolved. Moreover, we observe that the input label map has only a few semantic classes in the entire dataset. Thus the generator should focus more on learning these existing semantic classes rather than all the semantic classes. To tackle both limitations, we propose a novel semantic preserving module, which aims to selectively highlight class-dependent feature maps according to the input labels for generating semantically consistent images. We also propose a new similarity loss to model the intra-class and inter-class semantic dependencies.

Contrastive Learning. Recently, the most compelling methods for learning representations without labels have been unsupervised contrastive learning (Van den Oord et al., 2018; Hjelm et al., 2018; Pan et al., 2021; Wu et al., 2018; Chen et al., 2020), which significantly outperform other pretext task-based alternatives (Gidaris et al., 2018; Doersch et al., 2015; Noroozi & Favaro, 2016). Contrastive learning aims to learn the general features of a dataset without labels by teaching the model which data points are similar or different. For example, Pan et al. (2021) proposed VideoMoCo for unsupervised video representation learning. Chen et al. (2020) introduced a simple framework for contrastive learning of visual representations, which we call SimCLR. This paper proposes a novel pixel-wise contrastive learning method for semantic image synthsis in the fully supervised setting. It yields a new training protocol that explores global pixel relations in labeled layouts for regularizing the generation embedding space.

3 EDGE GUIDED GANS WITH CONTRASTIVE LEARNING

Framework Overview. Fig. 1 shows the overall structure of ECGAN for semantic image synthesis, which consists of a semantic and edge guided generator G and a multi-modality discriminator D. The generator G consists of eight components: (1) a parameter-sharing convolutional encoder E is proposed to produce deep feature maps F; (2) an edge generator G_e is adopted to generate edge maps $I_e^{'}$ taking as input deep features from the encoder; (3) an image generator G_i is used to produce intermediate images $I^{'}$; (4) an attention guided edge transfer module G_t is designed to forward useful structure information from the edge generator to the image generator; (5) the semantic preserving module G_s is developed to selectively highlight class-dependent feature maps according to the input label for generating semantically consistent images $I^{''}$; (6) a label generator G_l is employed to produce the label from $I^{''}$; (7) the similarity loss is proposed to calculate the intra-class and inter-class relationships. (8) the contrastive learning module G_c aims to model

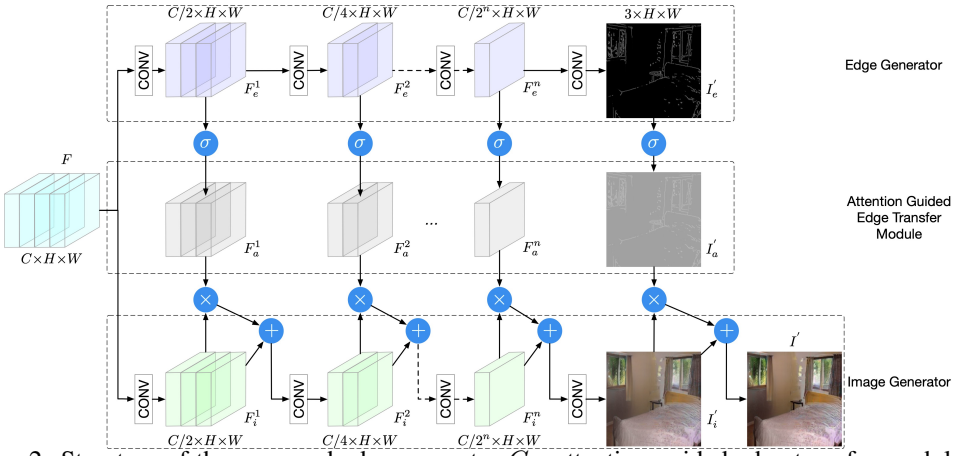

Figure 2: Structure of the proposed edge generator G_e, attention guided edge transfer module G_t, and image generator G_i. The edge generator G_e selectively transfers useful local structure information to the image generator G_i using the proposed attention guided transfer module G_t. The symbols $\oplus$, $\otimes$, and σ denote element-wise addition, element-wise multiplication, and Sigmoid activation function, respectively.

global semantic relations between training pixels, guiding pixel embeddings towards cross-image category-discriminative representations that eventually improve the generation performance.

Meanwhile, to effectively train the network, we propose a multi-modality discriminator D that distinguishes the outputs from both modalities, i.e., edge and image.

3.1 Edge Guided Semantic Image Synthesis

Parameter-Sharing Encoder. The backbone encoder E can employ any deep network architecture, e.g., the commonly used AlexNet (Krizhevsky et al., 2012), VGG (Simonyan & Zisserman, 2015), and ResNet (He et al., 2016). We directly utilize the feature maps from the last convolutional layer as deep feature representations, i.e., $F{=}E(S)$, where E represents the encoder; $S{\in}\mathbb{R}^{N\times H\times W}$ is the input label, with H and W as width and height of the input semantic labels, and N as the total number of semantic classes. Optionally, one can always combine multiple intermediate feature maps to enhance the feature representation. The encoder is shared by the edge generator and the image generator. Then, the gradients from the two generators all contribute to updating the parameters of the encoder. This compact design can potentially enhance the deep representations as the encoder can simultaneously learn structure representations from the edge generation branch and appearance representations from the image generation branch.

Edge Guided Image Generation. As discussed, the lack of detailed structure or geometry guidance makes it extremely difficult for the generator to produce realistic local structures and details. To overcome this limitation, we propose to adopt the edge as guidance. A novel edge generator G_e is designed to directly generate the edge maps from the input semantic labels. This also facilitates the shared encoder to learn more local structures of the targeted images. Meanwhile, the image generator G_i aims to generate photo-realistic images from the input labels. In this way, the encoder is boosted to learn the appearance information of the targeted images.

Previous works (Park et al., 2019; Liu et al., 2019; Qi et al., 2018; Chen & Koltun, 2017; Wang et al., 2018) directly use deep networks to generate the target image, which is challenging since the network needs to simultaneously learn appearance and structure information from the input labels. In contrast, the proposed method learns structure and appearance separately via the proposed edge generator and image generator. Moreover, the explicit guidance from the ground truth edge maps can also facilitate the training of the encoder.

The framework of both edge and image generators is illustrated in Fig. 2. Given the feature maps from the last convolutional layer of the encoder, i.e., $F{\in}\mathbb{R}^{C\times H\times W}$, where H and W are the width and height of the features, and C is the number of channels, the edge generator produces edge features and edge maps which are further utilized to guide the image generator to generate the interme-

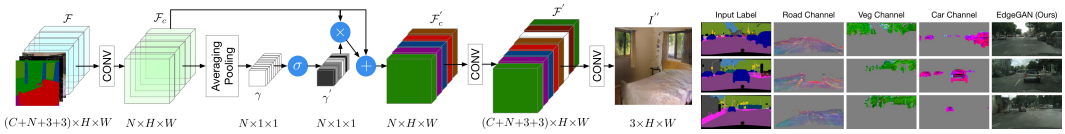

Figure 3: **Left:** Overview of the proposed semantic preserving module G_s, which aims at capturing the semantic information and predicts scaling factors conditioned on the combined feature maps $\mathcal{F}$. These learned factors selectively highlight class-dependent feature maps, which are visualized in different colors. The symbols $\oplus$, $\otimes$, and $\textcircled{\sigma}$ denote element-wise addition, element-wise multiplication, and Sigmoid activation function, respectively. **Right:** Visualization of three different feature channels in $\mathcal{F}^{'}$ on Cityscapes, i.e., road, car, and vegetation.

diate image $I^{'}$. The edge generator G_e contains n convolution layers and correspondingly produces n intermediate feature maps $F_e{=}\{F_e^j\}_{j=1}^n$. After that, another convolution layer with Tanh non-linear activation is utilized to generate the edge map $I_e^{'}{\in}\mathbb{R}^{3\times H\times W}$. Meanwhile, the feature maps F is also fed into the image generator G_i to generate n intermediate feature maps $F_i{=}\{F_i^j\}_{j=1}^n$. Then another convolution operation with Tanh non-linear activation is adopted to produce the intermediate image $I_i^{'}{\in}\mathbb{R}^{3\times H\times W}$. In addition, the intermediate edge feature maps F_e and the edge map $I_e^{'}$ are utilized to guide the generation of the image feature maps F_i and the intermediate image $I^{'}$ via the Attention Guided Edge Transfer as detailed below.

Attention Guided Edge Transfer. We further propose a novel attention guided edge transfer module G_t to explicitly employ the edge structure information to refine the intermediate image representations. The architecture of the proposed transfer module G_t is illustrated in Fig. 2. To transfer useful structure information from edge feature maps $F_e{=}\{F_e^j\}_{j=1}^n$ to the image feature maps $F_i{=}\{F_i^j\}_{j=1}^n$, the edge feature maps are firstly processed by a Sigmoid activation function to generate the corresponding attention maps $F_a{=}\text{Sigmoid}(F_e){=}\{F_a^j\}_{j=1}^n$. The attention aims to provide structural information (which cannot be provided by the input label map) within each semantic class. Then, we multiply the generated attention maps with the corresponding image feature maps to obtain the refined maps, which incorporate local structures and details. Finally, the edge refined features are element-wisely summed with the original image features to produce the final edge refined features, which are further fed to the next convolution layer as $F_i^j{=}\text{Sigmoid}(F_e^j){\times}F_i^j{+}F_i^j\,(j{=}1,\cdots,n)$. In this way, the image feature maps also contain the local structure information provided by the edge feature maps. Similarly, to directly employ the structure information from the generated edge map $I_e^{'}$ for image generation, we adopt the attention guided edge transfer module to refine the generated image directly with edge information as

$$I^{'} = \text{Sigmoid}(I_e^{'}) \times I_i^{'} + I_i^{'}, \tag{1}$$

where $I_a^{'}{=}\text{Sigmoid}(I_e^{'})$ is the generated attention map. We also provide the visualization results in Fig. 9.

3.2 Semantic Preserving Image Enhancement

Semantic Preserving Module. Due to the spatial resolution loss caused by convolution, normalization, and down-sampling layers, existing models (Wang et al., 2018; Park et al., 2019; Qi et al., 2018; Chen & Koltun, 2017) cannot fully preserve the semantic information of the input labels as illustrated in Fig. 7. For instance, the small 'pole' is missing, and the large 'fence' is incomplete. To tackle this problem, we propose a novel semantic preserving module, which aims to select class-dependent feature maps and further enhance it through the guidance of the original semantic layout. An overview of the proposed semantic preserving module G_s is shown in Fig. 3(left). Specifically, the input of the module denoted as $\mathcal{F}$, is the concatenation of the input label S, the generated intermediate edge map $I_e^{'}$ and image $I^{'}$, and the deep feature F produced from the shared encoder E. Then, we apply a convolution operation on $\mathcal{F}$ to produce a new feature map $\mathcal{F}_c$ with the number of channels equal to the number of semantic categories, where each channel corresponds to a specific semantic category (a similar conclusion can be found in (Fu et al., 2019)). Next, we apply the averaging pooling operation on $\mathcal{F}_c$ to obtain the global information of each class followed by a Sigmoid activation function to derive scaling factors $\gamma^{'}$ as in $\gamma^{'}{=}\text{Sigmoid}(\text{AvgPool}(\mathcal{F}_c))$, where each

value represents the importance of the corresponding class. Then, the scaling factor $\gamma^{'}$ is adopted to reweight the feature map $\mathcal{F}_c$ and highlight corresponding class-dependent feature maps as Eq. 2. The reweighted feature map is further added with the original feature $\mathcal{F}_c$ to compensate for information loss due to multiplication, and produces $\mathcal{F}_c^{'} \in \mathbb{R}^{N \times H \times W}$,

$$\mathcal{F}_c^{'} = \mathcal{F}_c \times \gamma^{'} + \mathcal{F}_c. \tag{2}$$

After that, we perform another convolution operation on $\mathcal{F}_c^{'}$ to obtain the feature map $\mathcal{F}^{'} \in \mathbb{R}^{(C+N+3+3) \times H \times W}$ to enhance the representative capability of the feature. In addition, $\mathcal{F}^{'}$ has the same size as the original input one $\mathcal{F}$, which makes the module flexible and can be plugged into other existing architectures without modifications of other parts to refine the output. In Fig. 3(right), we visualize three channels in $\mathcal{F}^{'}$ on Cityscapes, i.e., road, car, and vegetation. We can easily observe that each channel learns well the class-level deep representations.

Finally, the feature map $\mathcal{F}^{'}$ is fed into a convolution layer followed by a Tanh non-linear activation layer to obtain the final result $I^{''}$. Our semantic preserving module enhances the representational power of the model by adaptively recalibrating semantic class-dependent feature maps, and shares similar spirits with style transfer (Huang & Belongie, 2017), and recent works SENet (Hu et al., 2018) and EncNet (Zhang et al., 2018). One intuitive example of the utility of the module is for the generation of small object classes: the small object classes are easily missed in the generation results due to spatial resolution loss, while our scaling factor can put an emphasis on small objects and help preserve them.

Similarity Loss. It is hard for the network to preserve semantic information from isolated pixels. To explicitly regularize the framework to capture the relationship between semantic categories, we introduce a new similarity loss. For each pixel in the label, this loss forces the network to consider the pixels of the same category (intra-class) and the pixels among the different categories (inter-class). To this end, we first use a pretrained state-of-the-art model (i.e., SegFormer (Xie et al., 2021)) to tranfer the generated image $I^{''}$ back to a label $S^{''} \in \mathbb{R}^{N \times H \times W}$, with H and W as width and height, and N as the total number of semantic classes. A conventional method for addressing this problem is to use the cross entropy loss between $S^{''}$ and S. However, such a loss only considers the isolated pixel while ignoring the semantic correlation with other pixels.

To address this limitation, we construct a similarity map from $S \in \mathbb{R}^{N \times H \times W}$. Specifically, we reshape S to $\hat{S} \in N \times M$, in which $M = HW$. Next, we conduct the matrix multiplication to obtian a similarity map $A = \hat{S}\hat{S}^{\top} \in M \times M$, which encodes which pixels belong to the same category, i.e., if the j-*th* pixel and the i-*th* pixel belong to the same category, then the value of the j-*th* row and the i-*th* column in A is 1, otherwise it is 0. In the same way, we can obtain a similarity map $A^{''}$ from the label $S^{''}$. We then calculate the binary cross entropy loss between two similarity maps $\{a_m \in A, m \in [1, M^2]\}$ and $\{a_m^{''} \in A^{''}, m \in [1, M^2]\}$ as

$$\mathcal{L}_{sim}(S, S^{''}) = -\frac{1}{M^2} \sum_{m=1}^{M^2} (a_m \log a_m^{''} + (1 - a_m) \log(1 - a_m^{''})). \tag{3}$$

This similarity loss captures the intra-class and inter-class semantic correlation explicitly, leading to better generation results.

3.3 Contrastive Learning for Semantic Image Synthesis

Pixel-Wise Contrastive Learning. Existing semantic image synthesis models utilize deep architectures to project labeled pixels into a highly non-linear embedding space. However, they typically learn the embedding space that only makes use of 'local' context around pixel samples for a single input semantic layout (i.e., pixel dependencies within individual images) but ignores the 'global' context of the whole dataset (i.e., pixel semantic cross-relations across layouts). Hence, an important issue has been long ignored in the field: what should a good semantic image synthesis embedding space look like? Ideally, it should not only (i) address the categorization ability of individual pixel embeddings but also (ii) be well structured to address intra-class compactness and inter-class dispersion. With regard to (ii), pixels from a same class should to generate more similar image content than those from different classes, in the embedding space. Prior studies in representation learning

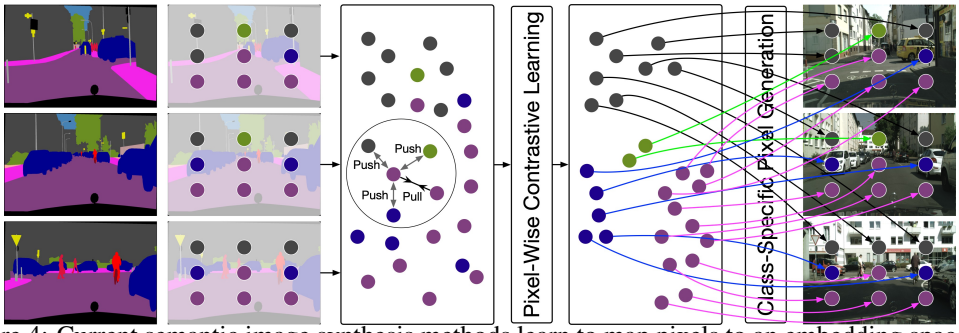

Figure 4: Current semantic image synthesis methods learn to map pixels to an embedding space but ignore intrinsic structures of labeled data (i.e., inter-layout relations among pixels from the same class, marked with the same color). We propose pixel-wise contrastive learning to foster a new training paradigm by explicitly addressing intra-class compactness and inter-class dispersion. Each pixel (embedding) is pulled closer to pixels of the same class but pushed far from pixels from other classes. Thus a better-structured embedding space is derived, eventually leading to the same class generating more similar image content and boosting the performance of semantic image synthesis.

also suggested that encoding intrinsic structures of training data would facilitate feature discriminativeness. So we speculate that, although existing algorithms have achieved impressive performance, it is possible to learn a better-structured pixel embedding space by considering both (i) and (ii).

Unsupervised visual representation learning aims to learn a CNN encoder that transforms each training semantic layout S to a feature vector $v = B(S) \in \mathbb{R}^D$, where B denotes the backbone network. In this way, v can best describe S. To achieve this goal, contrastive approaches conduct training by distinguishing a positive (an augmented version of anchor S) from several negatives, based on the principle of similarity between samples. A popular loss function for contrastive learning, called InfoNCE (Van den Oord et al., 2018; Gutmann & Hyvärinen, 2010), can be formulated in the following form:

$$\mathcal{L}_S^{NCE} = -\log \frac{\exp(v \cdot v^+/\tau)}{\exp(v \cdot v^+/\tau) + \sum_{v^- \in N_S} \exp(v \cdot v^-/\tau)}, \tag{4}$$

where v^+ is an embedding of a positive for S, N_S contains embeddings of negatives, '$\cdot$' denotes the inner (dot) product, and $\tau > 0$ is a temperature hyper-parameter. Note that all the embeddings in the loss function are L_2-normalized.

However, such training objective design mainly suffers from the limitation, i.e., it penalizes pixel-wise predictions independently but ignores cross-relationship between pixels. To solve this limitation, we develop a pixel-wise contrastive learning method which aims to regularizes the embedding space and explores the global structures of training data. Basically, the data samples in our contrastive loss computation are training semantic layout pixels. In addition, for a pixel i with its ground-truth semantic label $\bar{c}$, the positive samples are other pixels also belonging to the class $\bar{c}$, while the negatives are the pixels belonging to the other classes $C \backslash \bar{c}$. Thus, the proposed pixel-wise contrastive learning loss is defined as:

$$\mathcal{L}_i^{NCE} = \frac{1}{|P_i|} \sum_{i^+ \in P_i} -\log \frac{\exp(i \cdot i^+/\tau)}{\exp(i \cdot i^+/\tau) + \sum_{i^- \in N_i} \exp(i \cdot i^-/\tau)}, \tag{5}$$

where P_i and N_i denote pixel embedding collections of the positive and negative samples, respectively, for pixel i. Note that the positive/negative samples and the anchor i are not restricted to being from the same image. The purpose of such pixel-to-pixel contrastive learning based loss design is to learn an embedding space by pulling the same class pixel samples close and pushing different class samples apart. By doing so, pixels of the same class can generate closer image content than those of different classes.

Class-Specific Pixel Generation. As discussed in the introduction, the training data imbalance between different classes and the size difference between semantic objects makes it extremely difficult to generate small object classes and fine details. To address this, we propose a novel class-specific

Table 1: User study on Cityscapes, ADE20K, and COCO-Stuff. The numbers indicate the percentage of users who favor the results of the proposed method over the competing methods.

AMT ↑	Cityscapes	ADE20K	COCO-Stuff
Ours vs. CRN (Chen & Koltun, 2017)	88.8	94.8	95.3
Ours vs. Pix2pixHD (Wang et al., 2018)	87.2	93.6	93.9
Ours vs. SIMS (Qi et al., 2018)	85.3	-	-
Ours vs. GauGAN (Park et al., 2019)	84.7	88.4	90.8
Ours vs. DAGAN (Tang et al., 2020a)	81.8	86.2	-
Ours vs. CC-FPSE (Liu et al., 2019)	79.5	85.1	86.7
Ours vs. LGGAN (Tang et al., 2020b)	78.4	82.7	-
Ours vs. OASIS (Sushko et al., 2021)	76.7	80.6	82.5

pixel generation method. It can generate image content for each semantic class, thus being able to largely avoid the interference from large object classes during the joint optimization. Each sub-generation branch concentrates on a specific class, therefore being capable of effectively producing similar generation quality for different classes and yielding richer local image details.

An overview of the class-specific pixel generation method is provided in Fig. 4. After the proposed pixel-wise contrastive learning, we obtain a class-specific feature map for each pixel. Then, the feature map is fed into several convolutional layers for the corresponding semantic class, which generates an output image $\hat{I}_i$. To better learn each class, we utilize a pixel-wise $L1$ reconstruction loss, which can be expressed as follows:

$$\mathcal{L}_{\text{L1}} = \sum_{i=1}^{N} \mathbb{E}_{I_i, \hat{I}_i}[||I_i - \hat{I}_i||_1]. \tag{6}$$

The final output I_g from the pixel generation network can be obtained by performing an element-wise addition of all the class-specific outputs:

$$I_g = I_{g_1} \oplus I_{g_2} \oplus \cdots \oplus I_{g_N}. \tag{7}$$

We provide more training and implementation details of the proposed ECGAN in Appendix.

4 Experiments

Datasets. We follow GauGAN (Park et al., 2019) and conduct experiments on three datasets, i.e., Cityscapes (Cordts et al., 2016), ADE20K (Zhou et al., 2017), and COCO-Stuff (Caesar et al., 2018).

Evaluation Metrics. We follow (Park et al., 2019) and adopt the mean Intersection-over-Union (mIoU), Pixel Accuracy (Acc), and Fréchet Inception Distance (FID) (Heusel et al., 2017) as the evaluation metrics.

4.1 Comparisons with State-of-the-Art Methods

Qualitative Comparisons. We adopt GauGAN (Park et al., 2019) as the encoder E to validate the effectiveness of the proposed method. Visual comparison results on all the three datasets with the SOTA method are shown in Fig. 5. We can observe that the proposed ECGAN achieves visually better results with fewer visual artifacts than the SOTA method. For instance, on scene datasets such as Cityscapes and ADE20K, ECGAN generates sharper images than the baseline, especially at local structures and details, further verifying our motivation.

User Study. We follow the same evaluation protocol of GauGAN (Park et al., 2019) and conduct a user study. Specifically, we provide the participants an input semantic layout and two generated images from different models and ask them to choose the generated image that looks more like a corresponding image of the semantic layout. The users are given unlimited time to make the decision. The results of Cityscapes, ADE20K, and COCO-Stuff are shown in Table 1. We observe that users favor our synthesized results on all the three datasets compared with other competing methods, further validating that the generated images by the proposed method are more natural.

Quantitative Comparisons. Although the user study is more suitable for evaluating the quality of the generated images, we also follow previous works and use mIoU, Acc, and FID for quantitative

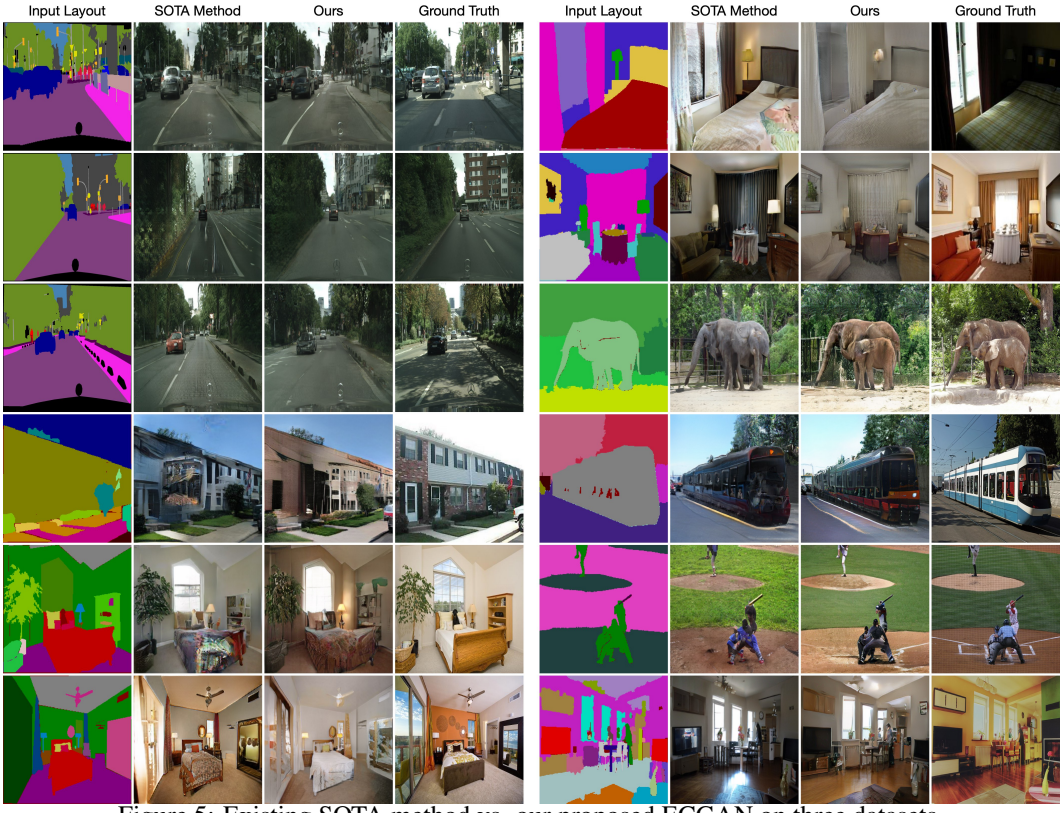

Figure 5: Existing SOTA method vs. our proposed ECGAN on three datasets.

Table 2: Quantitative comparison of different methods on Cityscapes, ADE20K, and COCO-Stuff.

Method	Cityscapes			ADE20K			COCO-Stuff		
	mIoU ↑	Acc ↑	FID ↓	mIoU ↑	Acc ↑	FID ↓	mIoU ↑	Acc ↑	FID ↓
CRN (Chen & Koltun, 2017)	52.4	77.1	104.7	22.4	68.8	73.3	23.7	40.4	70.4
SIMS (Qi et al., 2018)	47.2	75.5	49.7	-	-	-	-	-	-
Pix2pixHD (Wang et al., 2018)	58.3	81.4	95.0	20.3	69.2	81.8	14.6	45.8	111.5
DAGAN (Tang et al., 2020a)	66.1	82.6	60.3	40.5	81.6	31.9	-	-	-
LGGAN (Tang et al., 2020b)	68.4	83.0	57.7	41.6	81.8	31.6	-	-	-
CC-FPSE (Liu et al., 2019)	65.5	82.3	54.3	43.7	82.9	31.7	41.6	70.7	19.2
GauGAN (Park et al., 2019)	62.3	81.9	71.8	38.5	79.9	33.9	37.4	67.9	22.6
OASIS (Sushko et al., 2021)	69.3	-	47.7	48.8	-	28.3	44.1	-	17.0
ECGAN (Ours)	**72.2**	**83.1**	**44.5**	**50.6**	**83.1**	**25.8**	**46.3**	**70.5**	**15.7**

evaluation. The results of the three datasets are shown in Table 2. It is clear that the proposed method outperforms other leading methods by a large margin on all the three datasets, validating the effectiveness of the proposed method.

We provide more results and ablation study of the proposed ECGAN in Appendix.

5 Conclusion

We propose a novel ECGAN for semantic image synthesis. It introduces four core components: edge guided image generation strategy, attention guided edge transfer module, semantic preserving module, and contrastive learning module. The first one is employed to generate edge maps from input semantic labels. The second one is used to selectively transfer the useful structure information from the edge branch to the image branch. The third one is adopted to alleviate the problem of spatial resolution losses caused by different operations in the deep nets. The last one is utilized to investigate global semantic relations between training pixels, guiding pixel embeddings towards cross-image category-discriminative representations that eventually improve the generation performance. Extensive experiments on three datasets show that our method achieves significantly better results than existing models.

REFERENCES

Aayush Bansal, Yaser Sheikh, and Deva Ramanan. Shapes and context: in-the-wild image synthesis & manipulation. In *CVPR*, 2019. 3

David Bau, Hendrik Strobelt, William Peebles, Jonas Wulff, Bolei Zhou, Jun-Yan Zhu, and Antonio Torralba. Semantic photo manipulation with a generative image prior. *ACM TOG*, 38(4):1–11, 2019a. 1

David Bau, Jun-Yan Zhu, Hendrik Strobelt, Bolei Zhou, Joshua B Tenenbaum, William T Freeman, and Antonio Torralba. Gan dissection: Visualizing and understanding generative adversarial networks. In *ICLR*, 2019b. 1

Holger Caesar, Jasper Uijlings, and Vittorio Ferrari. Coco-stuff: Thing and stuff classes in context. In *CVPR*, 2018. 2, 8

John Canny. A computational approach to edge detection. *IEEE TPAMI*, (6):679–698, 1986. 14

Qifeng Chen and Vladlen Koltun. Photographic image synthesis with cascaded refinement networks. In *ICCV*, 2017. 1, 3, 4, 5, 8, 9

Ting Chen, Simon Kornblith, Mohammad Norouzi, and Geoffrey Hinton. A simple framework for contrastive learning of visual representations. In *ICML*, 2020. 3

Marius Cordts, Mohamed Omran, Sebastian Ramos, Timo Rehfeld, Markus Enzweiler, Rodrigo Benenson, Uwe Franke, Stefan Roth, and Bernt Schiele. The cityscapes dataset for semantic urban scene understanding. In *CVPR*, 2016. 2, 8, 15

Carl Doersch, Abhinav Gupta, and Alexei A Efros. Unsupervised visual representation learning by context prediction. In *ICCV*, 2015. 3

Jun Fu, Jing Liu, Haijie Tian, Yong Li, Yongjun Bao, Zhiwei Fang, and Hanqing Lu. Dual attention network for scene segmentation. In *CVPR*, 2019. 5

Spyros Gidaris, Praveer Singh, and Nikos Komodakis. Unsupervised representation learning by predicting image rotations. 2018. 3

Ian Goodfellow, Jean Pouget-Abadie, Mehdi Mirza, Bing Xu, David Warde-Farley, Sherjil Ozair, Aaron Courville, and Yoshua Bengio. Generative adversarial nets. In *NeurIPS*, 2014. 14

Shuyang Gu, Jianmin Bao, Hao Yang, Dong Chen, Fang Wen, and Lu Yuan. Mask-guided portrait editing with conditional gans. In *CVPR*, 2019. 1

Michael Gutmann and Aapo Hyvärinen. Noise-contrastive estimation: A new estimation principle for unnormalized statistical models. In *AISTATS*, 2010. 7

Kaiming He, Xiangyu Zhang, Shaoqing Ren, and Jian Sun. Deep residual learning for image recognition. In *CVPR*, 2016. 4

Martin Heusel, Hubert Ramsauer, Thomas Unterthiner, Bernhard Nessler, and Sepp Hochreiter. Gans trained by a two time-scale update rule converge to a local nash equilibrium. In *NeurIPS*, 2017. 8

R Devon Hjelm, Alex Fedorov, Samuel Lavoie-Marchildon, Karan Grewal, Phil Bachman, Adam Trischler, and Yoshua Bengio. Learning deep representations by mutual information estimation and maximization. In *ICLR*, 2018. 3

Jie Hu, Li Shen, and Gang Sun. Squeeze-and-excitation networks. In *CVPR*, 2018. 6

Xun Huang and Serge Belongie. Arbitrary style transfer in real-time with adaptive instance normalization. In *ICCV*, 2017. 6

Phillip Isola, Jun-Yan Zhu, Tinghui Zhou, and Alexei A Efros. Image-to-image translation with conditional adversarial networks. In *CVPR*, 2017. 1, 3

Liming Jiang, Changxu Zhang, Mingyang Huang, Chunxiao Liu, Jianping Shi, and Chen Change Loy. Tsit: A simple and versatile framework for image-to-image translation. In *ECCV*, 2020. 1

Diederik P Kingma and Jimmy Ba. Adam: A method for stochastic optimization. In *ICLR*, 2015. 14

Alex Krizhevsky, Ilya Sutskever, and Geoffrey E Hinton. Imagenet classification with deep convolutional neural networks. In *NeurIPS*, 2012. 4

Jingyuan Li, Fengxiang He, Lefei Zhang, Bo Du, and Dacheng Tao. Progressive reconstruction of visual structure for image inpainting. In *ICCV*, 2019. 3

Xihui Liu, Guojun Yin, Jing Shao, Xiaogang Wang, et al. Learning to predict layout-to-image conditional convolutions for semantic image synthesis. In *NeurIPS*, 2019. 1, 3, 4, 8, 9

Takeru Miyato, Toshiki Kataoka, Masanori Koyama, and Yuichi Yoshida. Spectral normalization for generative adversarial networks. In *ICLR*, 2018. 13

Kamyar Nazeri, Eric Ng, Tony Joseph, Faisal Qureshi, and Mehran Ebrahimi. Edgeconnect: Structure guided image inpainting using edge prediction. In *ICCV Workshops*, 2019a. 3

Kamyar Nazeri, Harrish Thasarathan, and Mehran Ebrahimi. Edge-informed single image super-resolution. In *ICCV Workshops*, 2019b. 3

Mehdi Noroozi and Paolo Favaro. Unsupervised learning of visual representations by solving jigsaw puzzles. In *ECCV*, 2016. 3

Evangelos Ntavelis, Andrés Romero, Iason Kastanis, Luc Van Gool, and Radu Timofte. Sesame: Semantic editing of scenes by adding, manipulating or erasing objects. In *ECCV*, 2020. 3

Tian Pan, Yibing Song, Tianyu Yang, Wenhao Jiang, and Wei Liu. Videomoco: Contrastive video representation learning with temporally adversarial examples. In *CVPR*, 2021. 3

Taesung Park, Ming-Yu Liu, Ting-Chun Wang, and Jun-Yan Zhu. Semantic image synthesis with spatially-adaptive normalization. In *CVPR*, 2019. 1, 3, 4, 5, 8, 9, 14

Xiaojuan Qi, Qifeng Chen, Jiaya Jia, and Vladlen Koltun. Semi-parametric image synthesis. In *CVPR*, 2018. 1, 3, 4, 5, 8, 9

Yurui Ren, Xiaoming Yu, Ruonan Zhang, Thomas H Li, Shan Liu, and Ge Li. Structureflow: Image inpainting via structure-aware appearance flow. In *ICCV*, 2019. 3

Karen Simonyan and Andrew Zisserman. Very deep convolutional networks for large-scale image recognition. In *ICLR*, 2015. 4, 13

Vadim Sushko, Edgar Schönfeld, Dan Zhang, Juergen Gall, Bernt Schiele, and Anna Khoreva. You only need adversarial supervision for semantic image synthesis. In *ICLR*, 2021. 3, 8, 9

Zhentao Tan, Menglei Chai, Dongdong Chen, Jing Liao, Qi Chu, Bin Liu, Gang Hua, and Nenghai Yu. Diverse semantic image synthesis via probability distribution modeling. In *CVPR*, pp. 7962–7971, 2021a. 3

Zhentao Tan, Dongdong Chen, Qi Chu, Menglei Chai, Jing Liao, Mingming He, Lu Yuan, Gang Hua, and Nenghai Yu. Efficient semantic image synthesis via class-adaptive normalization. *IEEE TPAMI*, 2021b. 3

Hao Tang, Dan Xu, Nicu Sebe, Yanzhi Wang, Jason J Corso, and Yan Yan. Multi-channel attention selection gan with cascaded semantic guidance for cross-view image translation. In *CVPR*, 2019. 13

Hao Tang, Song Bai, and Nicu Sebe. Dual attention gans for semantic image synthesis. In *ACM MM*, pp. 1994–2002, 2020a. 1, 8, 9

Hao Tang, Dan Xu, Yan Yan, Philip HS Torr, and Nicu Sebe. Local class-specific and global image-level generative adversarial networks for semantic-guided scene generation. In *CVPR*, 2020b. 3, 8, 9

Aaron Van den Oord, Yazhe Li, and Oriol Vinyals. Representation learning with contrastive predictive coding. *arXiv e-prints*, pp. arXiv–1807, 2018. 3, 7

Ting-Chun Wang, Ming-Yu Liu, Jun-Yan Zhu, Andrew Tao, Jan Kautz, and Bryan Catanzaro. High-resolution image synthesis and semantic manipulation with conditional gans. In *CVPR*, 2018. 1, 3, 4, 5, 8, 9

Zhirong Wu, Yuanjun Xiong, Stella X Yu, and Dahua Lin. Unsupervised feature learning via non-parametric instance discrimination. In *CVPR*, 2018. 3

Tete Xiao, Yingcheng Liu, Bolei Zhou, Yuning Jiang, and Jian Sun. Unified perceptual parsing for scene understanding. In *ECCV*, 2018. 14

Enze Xie, Wenhai Wang, Zhiding Yu, Anima Anandkumar, Jose M Alvarez, and Ping Luo. Segformer: Simple and efficient design for semantic segmentation with transformers. *NeurIPS*, 2021. 6

Saining Xie and Zhuowen Tu. Holistically-nested edge detection. In *ICCV*, 2015. 16

Fisher Yu, Vladlen Koltun, and Thomas Funkhouser. Dilated residual networks. In *CVPR*, 2017. 14

Hang Zhang, Kristin Dana, Jianping Shi, Zhongyue Zhang, Xiaogang Wang, Ambrish Tyagi, and Amit Agrawal. Context encoding for semantic segmentation. In *CVPR*, 2018. 6

Bolei Zhou, Hang Zhao, Xavier Puig, Sanja Fidler, Adela Barriuso, and Antonio Torralba. Scene parsing through ade20k dataset. In *CVPR*, 2017. 2, 8

Peihao Zhu, Rameen Abdal, Yipeng Qin, and Peter Wonka. Sean: Image synthesis with semantic region-adaptive normalization. In *CVPR*, 2020a. 3

Zhen Zhu, Zhiliang Xu, Ansheng You, and Xiang Bai. Semantically multi-modal image synthesis. In *CVPR*, 2020b. 3

Appendix

A Model Training

Multi-Modality Discriminator. To facilitate the training of the proposed method for high-quality edge and image generation, a novel multi-modality discriminator is developed to simultaneously distinguish outputs from two modality spaces, i.e., edge and image. Since the edges and RGB images share the same structure, they can be learned using the multi-modality discriminator. In the preliminary experiment, we also tried to use two discriminators (i.e., an edge discriminator and an image discriminator), but no performance improvement was observed while increasing the model complexity. Thus, we use the proposed multi-modality discriminator. The framework of the multi-modality discriminator is shown in Fig. 1, which is capable of discriminating both real/fake images and edges. To discriminate real/fake edges, the discriminator loss considering the semantic label S and the generated edge $I_e^{'}$ (or the real edge I_e) is as Eq. 8 which guides the model to distinguish real edges from fake generated edges.

$$\mathcal{L}_{\text{CGAN}}(G_e, D) = \mathbb{E}_{S,I_e}\left[\log D(S, I_e)\right] + \mathbb{E}_{S,I_e^{'}}\left[\log(1 - D(S, I_e^{'}))\right]. \tag{8}$$

Further, to discriminate real/fake images, the discriminator loss regarding semantic label S and the generated images $I^{'}$, $I^{''}$ (or the real image I) is as Eq. 9, which guides the model to discriminate real/fake images.

$$\begin{aligned}\mathcal{L}_{\text{CGAN}}(G_i, G_s, D) &= (\lambda + 1)\mathbb{E}_{S,I}\left[\log D(S, I)\right] \\ &+ \mathbb{E}_{S,I^{'}}\left[\log(1 - D(S, I^{'}))\right] + \lambda\mathbb{E}_{S,I^{''}}\left[\log(1 - D(S, I^{''}))\right],\end{aligned} \tag{9}$$

where λ controls the losses of the two generated images. The inclusion of I' and I'' is a cascaded coarse-to-fine generation strategy (Tang et al., 2019), i.e., I' is the coarse result, while I'' is the refined result. The intuition is that I'' will be better generated based on I', so we provide I' to the discriminator to ensure that I' is also realistic.

Optimization Objective. Equipped with the multi-modality discriminator, we elaborate on the training objective for the proposed method as follows. Five different losses, i.e., the multi-modality adversarial loss, the similarity loss, the contrastive learning loss, the discriminator feature matching loss $\mathcal{L}_f$, and the perceptual loss $\mathcal{L}_p$ are used to optimize the proposed ECGAN,

$$\begin{aligned}\min_G \max_D \mathcal{L} = \lambda_c &\underbrace{(\mathcal{L}_{\text{CGAN}}(G_e, D) + \mathcal{L}_{\text{CGAN}}(G_i, G_s, D))}_{\text{Multi-Modality Adversarial Loss}} + \lambda_s \underbrace{\mathcal{L}_{sim}(S, S^{'}) + \mathcal{L}_{sim}(S, S^{''})}_{\text{Similarity Loss}} \\ &+ \lambda_l \underbrace{\mathcal{L}_i^{NEC} + \mathcal{L}_{L1}}_{\text{Contrastive Learning Loss}} + \lambda_f \underbrace{(\mathcal{L}_f(I_e, I_e^{'}) + \mathcal{L}_f(I, I^{'}) + \lambda\mathcal{L}_f(I, I^{''}))}_{\text{Discriminator Feature Matching Loss}} \\ &+ \lambda_p \underbrace{(\mathcal{L}_p(I_e, I_e^{'}) + \mathcal{L}_p(I, I^{'}) + \lambda\mathcal{L}_p(I, I^{''}))}_{\text{Perceptual Loss}},\end{aligned} \tag{10}$$

where λ_c, λ_s, λ_l, λ_f, and λ_p are the parameters of the corresponding loss that contributes to the total loss $\mathcal{L}$; where $\mathcal{L}_f$ matches the discriminator intermediate features between the generated images/edges and the real images/edges; where $\mathcal{L}_p$ matches the VGG (Simonyan & Zisserman, 2015) extracted features between the generated images/edges and the real images/edges. By maximizing the discriminator loss, the generator is promoted to simultaneously generate reasonable edge maps that can capture the local-aware structure information and generate photo-realistic images semantically aligned with the input semantic labels.

B Implementation Details

For both the image generator G_i and edge generator G_e, the kernel size and padding size of convolution layers are all 3×3 and 1 for preserving the feature map size. We set n=3 for generators G_i, G_s, and G_t. The channel size of feature F is set to C=64. For the semantic preserving module G_s, we adopt an adaptive average pooling operation. Spectral normalization (Miyato et al., 2018)

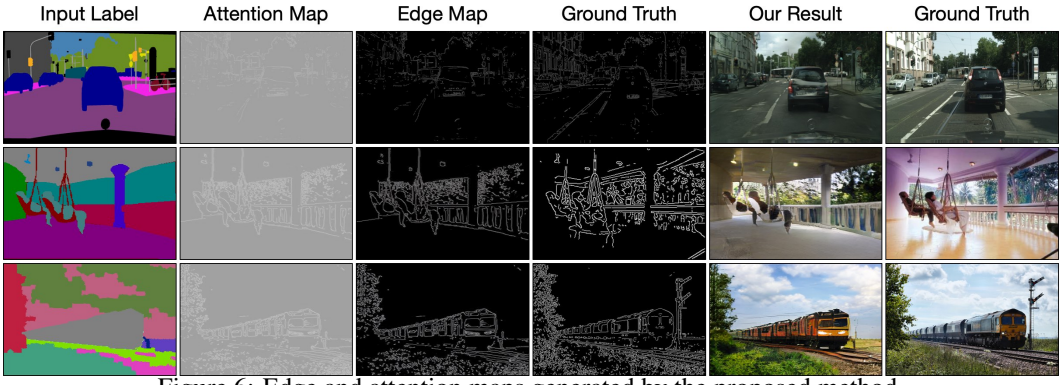

Figure 6: Edge and attention maps generated by the proposed method.

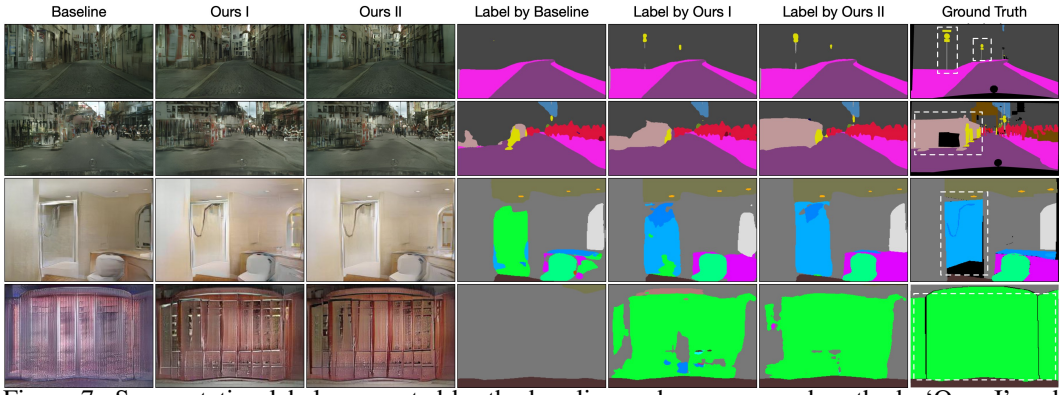

Figure 7: Segmentation labels generated by the baseline and our proposed method. 'Ours I' and 'Ours II' stand for $I^{'}$ and $I^{''}$, respectively.

is applied to all the layers in both the generator and discriminator. We adopt the Canny edge detector (Canny, 1986) to extract ground truth edge maps for training. Also, we follow the training procedures of GANs (Goodfellow et al., 2014) and alternatively train the generator G and discriminator D, i.e., one gradient descent step on discriminator and generator alternately. We use the Adam solver (Kingma & Ba, 2015) and set β_1=0, β_2=0.999. λ_c, λ_s, λ_l, λ_f, and λ_p in Eq. 10 is set to 1, 1, 1, 10, and 10, respectively. All λ in both Eq. 9 and 10 are set to 2. We conduct the experiments on an NVIDIA DGX1 with 8 V100 GPUs.

C More Results

Visualization of Edge and Attention Maps. We also visualize the generated edge and attention maps in Fig. 6. We observe that the proposed method can generate reasonable edge maps according to the input labels. Thus the generated edge maps can be used to provide more local structure information for generating more photo-realistic images.

Visualization of Segmentation Maps. We follow GauGAN and apply pre-trained segmentation networks (Yu et al., 2017; Xiao et al., 2018) on the generated images to produce segmentation maps. Results compared with the baseline method are shown in Fig. 7. We observe that the proposed method consistently generates better semantic labels than the baseline on both datasets.

Multi-Modal Image and Edge Synthesis. We follow GauGAN and apply a style encoder and a KL-Divergence loss with loss weight 0.05 to enable multi-modal image and edge synthesis in Fig. 8. Our model generates different edges and images from the same input layout, which we believe will benefit other tasks, e.g., image inpainting and super-resolution. Note that existing methods (e.g., (Park et al., 2019)) can only achieve multi-modal image synthesis.

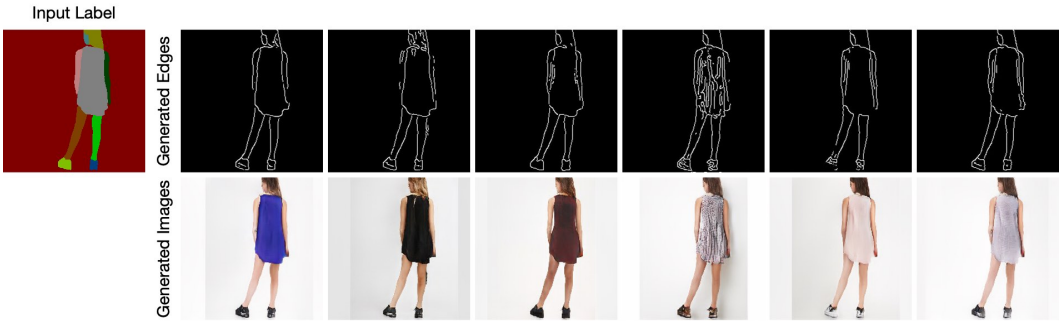

Figure 8: Results generated by the proposed method for multi-modal image and edge synthesis.

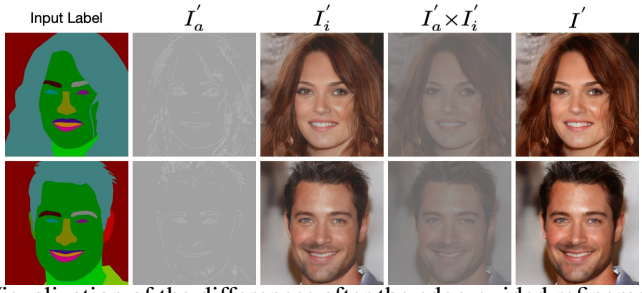

Figure 9: Visualization of the differences after the edge-guided refinement in Eq. 1.

Setting	mIoU ↑	Acc ↑	FID ↓
E+G_i	58.6	81.4	65.7
E+G_i+G_e	60.2	81.7	61.0
E+G_i+G_e+G_t	61.5	82.0	59.0
E+G_i+G_e+G_t+G_s	64.5	82.5	57.1
E+G_i+G_e+G_t+G_s+G_l	66.8	82.7	52.2
E+G_i+G_e+G_t+G_s+G_l+G_c	72.2	83.1	44.5

Table 3: Ablation study of the proposed method on Cityscapes.

D Ablation Study

Baseline Models. We conduct extensive ablation studies on Cityscapes (Cordts et al., 2016) to evaluate different components of the proposed method. Our method has six baselines as shown in Table 3: (1) 'E+G_i' means only using the encoder E and the proposed image generator G_i to synthesize the targeted images; (2) 'E+G_i+G_e' means adopting the proposed image generator G_i and edge generator G_e to simultaneously produce both edge maps and images; (3) 'E+G_i+G_e+G_t' connects the image generator G_i and the edge generator G_e by using the proposed attention guided edge transfer module G_t; (4) 'E+G_i+G_e+G_t+G_s' employs the proposed semantic preserving module G_s to further improve the quality of the final results. (5) 'E+G_i+G_e+G_t+G_s+G_l' uses the proposed label generator G_l to produce the label from the generated image, and then calculate the similarity loss between the generated label and the real one. (6) 'E+G_i+G_e+G_t+G_s+G_l+G_c' is our full model and uses the proposed pixel-wise contrastive learning and class-specific pixel generation methods to capture more semantic relations by explicitly exploring the structures of labelled pixels from multiple input semantic layouts.

Effect of Edge Guided Generation Strategy. The results are shown in Table 3. When using the edge generator G_e to produce the corresponding edge map from the input label, performance on all evaluation metrics is improved. Specifically, 1.6, 0.3, and 4.7 point gains on the mIoU, Acc, and FID metrics, respectively, which confirms the effectiveness of our edge guided generation strategy. We also provide several visualization results of the differences (see Eq. 1) after the edge-guided refinement in Fig. 9.

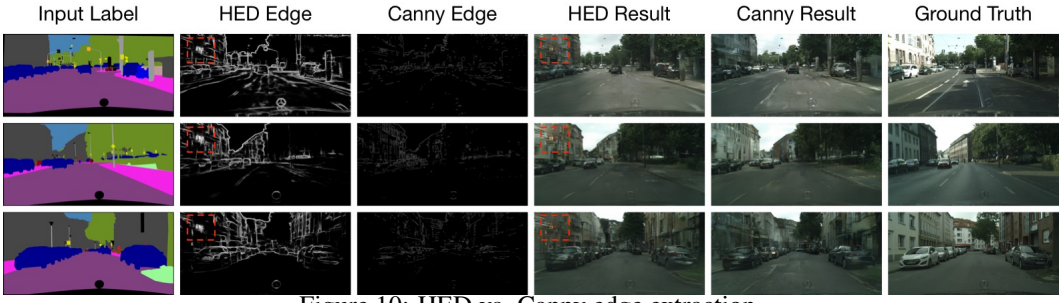

Figure 10: HED vs. Canny edge extraction.

Effect of Attention Guided Edge Transfer Module. We observe that the implicitly learned edge structure information by the 'E+G_i+G_e' baseline is not enough for such a challenging task. Thus we further adopt the transfer module G_t to transfer useful edge structure information from the edge generation branch to the image generation branch. We observe that 1.3, 0.3, and 2.0 point gains are obtained on the mIoU, Acc, and FID metrics, respectively. This means that G_t indeed learns rich feature representations with more convincing structure cues and details and then transfers them from G_e to G_i.

Effect of Semantic Preserving Module. By adding G_s, the overall performance is further boosted with 3.0, 0.5, and 1.9 point improvements on the mIoU, Acc, and FID metrics, respectively. This means G_s indeed learns and highlights class-specific semantic feature maps, leading to better generation results. In Fig. 7, we show some samples of the generated semantic maps. We observe that the semantic maps produced by the results with G_s (i.e., 'Label by Ours II' in Fig. 7) are more accurate than those without using G_s ('Label by Ours I' in Fig. 7). Moreover, we visualize three channels in $\mathcal{F}^{'}$ on Cityscapes in Fig. 3(right), i.e., road, car, and vegetation. Each channel learns well the class-level deep representations.

Effect of Similarity Loss. By adding the proposed label generator G_l and similarity loss, the overall performance is further boosted on all the three metrics. This means the proposed similarity loss indeed captures more intra-class and inter-class semantic dependencies, leading to better semantic layouts in the generated images.

Effect of Edge Extraction Methods. We also conduct experiments on Cityscapes with HED (Xie & Tu, 2015), leading the following results: 56.7 (FID), 64.5 (mIoU), and 82.3 (Acc), which are slightly worse than the results of Canny in Table 3. The reason is that the edges from HED are very thick and cannot accurately represent the edge of objects. It also ignores some local details since it focuses on extracting the contours of objects. Thus, HED is unsuitable for our setting as we aim to generate more local details/structures. Moreover, we see that the generated HED edges contain artifacts as indicated in the red boxes, which makes the generated images tend to have blurred edges (Fig. 10).

Effect of Contrastive Learning. When adopting the proposed pixel-wise contrastive learning and class-specific pixel generation methods to produce the results, the performance is significantly improved on all three datasets on all the three evaluation metrics. This means that the model does indeed learn a more discriminative class-specific feature representation, confirming the superiority of our design.